HHS Public Access

Author manuscript

Dev Neurosci. Author manuscript; available in PMC 2018 August 05.

Published in final edited form as:

Dev Neurosci. 2017 ; 39(6): 443–459. doi:10.1159/000477898.

Neuroprotective effects of intranasal IGF-1 against neonatal lipopolysaccharide-induced neurobehavioral deficits and neuronal inflammation in the substantia nigra and locus coeruleus of juvenile rats

Lu-Tai Tien[a], **Yih-Jing Lee**[a], **Yi Pang**[b], **Silu Lu**[b], **Jonathan W Lee**[b], **Chih-Hsueh Tseng**[a], **Abhay J Bhatt**[b], **Renate D Savich**[b], and **Lir-Wan Fan**[b,*]

[a]School of Medicine, Fu Jen Catholic University, Xinzhuang Dist, New Taipei City 24205, Taiwan

[b]Department of Pediatrics, Division of Newborn Medicine, University of Mississippi Medical Center, Jackson, MS 39216, USA

Abstract

Neonatal lipopolysaccharide (LPS) exposure-induced brain inflammation resulted in motor dysfunction and brain dopaminergic neuronal injury, and increased the risks of neurodegenerative disorders in adult rats. Our previous studies showed that intranasal administration of insulin-like growth factor-1 (IGF-1) protects against LPS-induced white matter injury in the developing rat brain. To further examine whether IGF-1 protects against LPS-induced brain neuronal injury and neurobehavioral dysfunction, recombinant human IGF-1 (rhIGF-1) at a dose of 50 μg/pup was administered intranasally 1 hour following intracerebral injection of LPS (1 mg/kg) in postnatal day 5 (P5) Sprague-Dawley rat pups. Neurobehavioral tests were carried out from P7 to P21, and brain neuronal injury was examined at P21. Our results showed that LPS exposure resulted in disturbances of motor behaviors in juvenile rats. Moreover, LPS exposure caused injury to central catecholaminergic neurons, as indicated by reduction of tyrosine hydroxylase (TH) immunoreactivity in the substantia nigra (SN), ventral tegmental area (VTA) and olfactory bulb (OB), and brain noradrenergic neurons, as indicated by reduction of TH immunoreactivity in the locus coeruleus (LC) of the P21 rat brain. The LPS-induced reduction of TH+ cells were observed at a greater degree in the SN and LC of the P21 rat brain. Intranasal rhIGF-1 treatment attenuated LPS-induced central catecholaminergic neuronal injury and motor behavioral disturbances, including locomotion, beam walking test and gait analysis. Intranasal rhIGF-1 administration also attenuated LPS-induced elevation of IL-1β levels and numbers of activated microglia, and cyclooxygenase-2+ cells, which were double labeled with TH+ cells in the SN, VTA, OB and LC of the P21 rat brain. These results suggest that IGF-1 may provide protection against neonatal LPS exposure-induced central catecholaminergic neuronal injury and motor behavioral disturbances, and that the protective effects are associated with the inhibition of microglia activation and the

*Corresponding author: Lir-Wan Fan, Ph.D. Associate Professor, Department of Pediatrics; Division of Newborn Medicine, University of Mississippi Medical Center, Jackson, MS 39216-4505, USA, Tel.: +1-601-984-2345; Fax: +1-601-815-3666: lwfan@umc.edu (LW Fan).

Conflict of interest: The authors declare that there are no conflicts of interest.

reduction of neuronal oxidative stress by the suppression of the neuronal cyclooxygenase-2 expression.

Keywords

Lipopolysaccharide; Neuroinflammation; Insulin-like growth factor-1; Microglia; Cyclooxygenase-2; Substantia nigra; Ventral tegmental area; Locus coeruleus

Introduction

Increasing evidence has indicated that perinatal infection/inflammation not only is a major contributor to brain injury in newborns, but also has long-term consequences and could speculatively modify the risk of a variety of neurological disorders in children and adults. Perinatal exposure to an endotoxin, lipopolysaccharide (LPS), a component of the cell wall of gram-negative bacteria [1], has been shown to increase the risk of dopaminergic disorders in animal models of Parkinson's disease [2, 3]. In our previous studies, we developed a neonatal rat model of central exposure to LPS through an intracerebral (i.c.) injection in postnatal day 5 (P5) rats (the brain development at P2-P7 rats are compatible with preterm infants at 23-32 gestation weeks) [4] to study nigrostriatal dopaminergic neuronal injury associated with the infection/inflammation in the immature brain [2, 5, 6]. Neonatal LPS treatment causes functional disability, such as sensory, motor, emotional and cognitive impairment in juvenile rats (P21), suggesting possible involvement of dopaminergic impairment in this neonatal rat model of central inflammation-induced neurological dysfunction [5, 6].

Insulin-like growth factor-1 (IGF-1) is a trophic factor produced in the liver and the central nervous system including neurons and glial cells [7]. The IGF-1 level in cerebral spinal fluid (CSF) is greater during early brain development, which indicates an important role in brain development, neuronal growth promotion, cellular proliferation and differentiation, especially during myelination and synapse formation in the developing nervous system [8, 9]. IGF-1 also has autocrine functions in the brain and contributes to the control of neuronal excitability, nerve cell metabolism and cell survival [10]. Therefore, IGF-1 is considered to have multiple neuroprotective properties in the adult brain [10, 11]. In addition, IGF-1 shows anti-inflammatory action by the reduction of LPS-induced brain cytokine expression via the down-regulating of glia activation and inducing of an endogenous growth factor [12, 13]. Intranasal administration provides a non-invasive method which may bypass the blood-brain barrier (BBB) to deliver therapeutic agents to the central nervous system, and thus reducing systemic exposure and side effects [14, 15]. Studies by us and others have shown that IGF-1 can be delivered to the rodent brain along olfactory and trigeminal pathways with intranasal administration [14, 15], and that intranasally delivered IGF-1 protects against LPS-induced white matter injury in the developing rat brain [16], cerebral hypoxic-ischemic injury [17–19], and other neurodegenerative damages [20, 21] which may be related to activation of intracellular signaling cascades such as the phophatidylinositol-3 kinase (PI3K)/Akt pathway [20, 23].

Our previous studies have revealed that neonatal exposure to LPS at P5 in rats produces chronic inflammation and injury in the nigrostriatal dopaminergic system [5, 6]. The LPS-induced neuroinflammation and neurobehavioral dysfunction are involved not only in the substantia nigra (SN) [23, 24], but also in other central catecholaminergic neurons such as the dopaminergic neurons in the ventral tegmental area (VTA) of midbrain [23, 25] and olfactory bulb (OB) [26, 27], and the noradrenergic neurons in the locus coeruleus (LC) of the pons [23, 24]. The objective of the present study is to further examine whether IGF-1 delivered through intranasal route in the neonatal rat provides long-lasting protection against LPS-induced dopaminergic and noradrenergic neuronal injury, and ameliorates LPS-induced neurobehavioral dysfunction in juvenile rats.

Materials and methods

Chemicals

Unless otherwise stated, all chemicals used in this study were purchased from Sigma (St. Louis, MO., USA). Recombinant human IGF-1 (rhIGF-1) was purchased from R&D Systems (Minneapolis, MN, USA). Monoclonal mouse antibodies against neuron-specific nuclear protein (NeuN) and tyrosine hydroxylase (TH) were purchased from Millipore (Billerica, MA, USA). Polyclonal goat antibodies against cyclooxygenase-2 (COX-2) and polyclonal rabbit antibodies against ionized calcium binding adapter molecule 1 (Iba1) were obtained from Santa Cruz Biotechnology (Santa Cruz, CA, USA) and Wako Chemicals USA (Irvine, CA, USA), respectively. ELISA kits for immunoassay of rat interleukin-1p (IL-1β), interleukin-6 (IL-6), and tumor necrosis factor-α (TNFα) were purchased from R&D Systems (Minneapolis, MN, USA).

Animals

Timed pregnant Sprague-Dawley rats arrived in the laboratory on day 19 of gestation. Animals were maintained in an animal room on a 12-h light/dark cycle and at constant temperature (22 ± 2°C). The day of birth was defined as postnatal day 0 (P0). After birth, the litter size was adjusted to ten pups per litter to minimize the effect of litter size on body weight and brain size. All procedures for animal care were conducted in accordance with the National Institutes of Health Guide for the Care and Use of Laboratory Animals and were approved by the Institutional Animal Care and Use Committee at the University of Mississippi Medical Center. Every effort was made to minimize the number of animals used and their suffering.

Surgery procedures and animal treatment

Intracerebral injection of LPS to 5-day old Sprague-Dawley rat pups of both sexes was performed as previously described [5, 16]. Under light anesthesia with isoflurane (1.5%), LPS (1 mg/kg, from Escherichia coli, serotype 055: B5) in sterile saline (total volume of 2 μl) was administered to the rat brain unilaterally at the location of 1.0 mm posterior and 1.0 mm left of the bregma, and 2.0 mm deep to the skull surface in a stereotaxic apparatus with a neonatal rat adapter. The dose of LPS was chosen based on the previously reported results which produced brain injury [5, 16]. The injection site was located at the area just above the left cingulum. The control rats were injected with the same volume of sterile saline. All

animals survived the intracerebral injection. Each dam had the same litter size (10 pups) and equal numbers of LPS-treated and saline-treated rat pups were included in a litter.

Intranasal administration of rhIGF-1 in the rat pup 1 hr following intracerebral injection of LPS or saline was performed as previously described [16, 17]. Briefly, P5 SD rat pups were placed on their backs under light anesthesia with isoflurane (5% for induction and 1.5% for maintenance). After pups were sedated, 50 μg of rhIGF-1 dissolved in 5 μl PBS containing 0.1% BSA was given into the left naris using a fine tip. This dose of IGF-1 has been shown to protect the neonatal rat brain from LPS-induced white matter injury [16] and hypoxic-ischemic injury in our previous studies [17]. The pups remained sedated with isoflurane for 5 min to ensure that they stayed on their backs. All pups woke up within 1-2 min upon withdrawal of isoflurane and were returned to their dams. For pups in the control group, 0.1% BSA was given by intranasal administration.

One animal from each litter was included in each experimental group. Twelve pups were included in each treatment group for behavioral tests. One or sixteen days following the injection (P6 or P21), 6 pups of each group were sacrificed by decapitation for fresh brain tissue collection. One set of animals at P21 was sacrificed by transcardiac perfusion with normal saline followed by 4% paraformaldehyde for brain section preparation. Free-floating coronal brain sections at 40 μm of thickness were prepared in a sliding microtome for immunohistochemistry staining and stereological estimates of the total number of neurons in the SN, VTA, OB and LC.

Behavioral testing

The motor behavioral tests, including locomotion and stereotypy, gait analysis and beam walking tests were performed by an investigator blind to the treatment as described previously [2, 5, 6] with modifications.

Locomotion and stereotypy—The open field test measures the activity and habituation response of animals on placement in a novel environment [28]. Locomotor activity was measured using the ANY-maze Tracking System (Stoelting Co., Wood Dale, IL, USA). Animals were placed in the activity chambers ($42 \times 25 \times 40$ cm^3) in a quiet room with dimmed light every other day from P9 to P21. The total distance traveled by the animal was recorded during a 10-min testing period. The number of rearing events were counted during the first 5-min testing period at P14 and P21. The summation of rearing responses and stereotyped behaviors reflect vertical activity which has been used apart from locomotion as a reliable criterion for motor activity during their exposure to novelty [29]. The stereotyped behaviors of standing, grooming, scratching, head-swinging, sniffing and freezing were quantified during the first 5-min testing period at P14 and P21. Quantification of stereotyped behaviors was achieved by counting the frequency of discrete episodes and the summation of all stereotyped responses during the testing period was scored for each rat [29].

Beam walking test—Motor coordination and balance were assessed by measuring the ability of the animals to traverse a narrow beam to reach an enclosed safety platform [30]. A 60 cm-long round wood beam with a diameter of 3 cm was placed horizontally, 50 cm above the bench surface, with one end mounted on a narrow support and the other end attached to a

goal box with a litter of pups. A sawdust-filled box that was placed underneath served as protection for the falling pups. A light (60 W) was positioned above the start of the beam. A litter of pups was placed in the goal box, and one pup at a time was removed and placed on the starting platform. Each pup was given three trials a day. The time spent on the beam for each pup that traversed the beam and joined their littermates was recorded and the cut-off time was 60 s.

Gait analysis—Gait abnormalities and beam walking deficits have been conducted for evaluation of nigrostriatal lesion in rodent models [31]. The hind paws of each rat were smeared with ink. The animal was allowed to walk up a runway (80×10 cm) covered with white paper that had a darkened part at the end. For motivational purposes, a white light (60 Watts) was placed at the beginning of the ramp. The walking task was repeated until four satisfactory walks of at least 4 steps without pause were obtained. Four variables from footprint pattern were measured as follows: (1) foot length (the length of hind foot), (2) spreading of toes 1–5 (the length between toes 1–5 of hind foot), (3) stride length (distance between the successive placement of the same hind foot), and (4) stride width (the vertical distance between one hind foot and the succeeding print of the opposite hind foot).

Immunohistochemistry studies

Free-floating coronal brain sections at 40 μm of thickness were prepared in a freezing microtome (Leica, SM2010R, Wetzlar, Germany). Primary antibodies were used with the following dilutions: NeuN (1:300), TH (1:1000), COX-2 (1:100) and Iba1 (1:500). NeuN detects the neuron-specific nuclear protein which primarily localizes in the nucleus of the neurons with slight staining in the cytoplasm. TH (the rate-limiting synthetic enzyme for dopamine and norepinephrine) was used to detect dopaminergic neurons in the SN, VTA and OB, and noradrenergic neurons in the LC. COX-2 provides selective staining of inducible cyclooxygenase. Microglia were detected using Iba1 immunostaining, which recognizes both the resting and the activated microglia. Sections were incubated with primary antibodies at 4 °C overnight and further incubated with secondary antibodies conjugated with fluorescent dyes (Alexa Fluor 488 or Alexa Fluor 555, Millipore, Billerica, MA, USA; and Cy2 or Cy3, Jackson Immunoresearch, West Grove, PA, USA) for 1 hr in the dark at room temperature. DAPI (100 ng/ml) was used simultaneously to stain nuclei and aid their identification during the final visualization. Sections incubated in the absence of primary antibody were used as negative controls. The resulting sections were examined under a fluorescent microscope (Nikon Ni-E, Melville, NY, USA, or Olympus BX60, Center Valley, PA, USA) at appropriate wavelengths.

Stereological estimates of the total number of cells in the brain

The stereological estimates of the total number of TH+ neurons, NeuN+ neurons, COX-2+ cells and Iba1+ cells in four reference spaces (SN, VTA, OB and LC) were performed in the P21 rat brain following the methods described previously [2, 3, 32]. Eight or four equally spaced thick sections (40 μm) in the midbrain and forebrain levels or pontine level that were to be used in the analysis came from a one in six series. The total number of TH+, NeuN+, COX-2+ or Iba1+ labeled cells (*est N*) were counted in each of the eight or four sections, which cover the entire SN, VTA, OB, or LC region, respectively. We found in our previous

study that FITC-labeled LPS administered through a unilateral i.c. injection distributed quickly to both hemispheres within 0.5 hr (data not shown). Furthermore, following a unilateral i.c. injection of LPS or saline in the P5 rat brain, no significant differences in density of TH+ cells were observed between the ipsilateral (left) and the contralateral side (right) of the P21 rat brain [5]. Therefore, stereological cell counting from both sides of the rat brain were averaged and presented in the present study. Stereological cell counting in the present study was focused in the SN region (nucleus A9 cells or cells in both the SN pars compacta and the SN pars reticulata), VTA region (nucleus A10 cells or cells in VTA), OB region (nucleus A16 cells or cells in OB) and LC region (nucleus A6 cells or cells in LC). The Cavalieri principle [33] was used to estimate the reference volumes, *est V(ref)*, and the volume density, *est* N_V. The product of the two is an estimate of the total number of cells in this region: *est V(ref)* × *est* N_V = *est N* [3, 33]. As described previously [32], the images were taken under unbiased conditions using Stereo Investigator software (MBF Bioscience, Williston, VT, USA) with a motorized microscope (Nikon Ni-E, Melville, NY, USA). Imaged cells were then examined and quantified with the software.

ELISA

Concentrations of IL-1β, IL-6 and TNFα in the rat brain at 24 hr or 16 days after the LPS exposure were determined as markers of LPS-induced inflammatory responses by ELISA. ELISA was performed following the manufacturer's instruction as previously described [16]. Briefly, brain tissues were homogenized in 5 volumes of ice-cold PBS (pH 7.2) and centrifuged at 12,000 g for 20 min, at 4°C. The supernatant was then collected and total protein was determined by the Bradford method. Data were acquired using a 96-well plate reader (Bio-Tek instruments, Inc., VT, USA). The cytokine concentrations are expressed as pg cytokine/mg protein.

Statistics

The locomotor, stereotyped and beam walking behavioral data were presented as the mean ±standard error of the mean (SEM) and analyzed by two-way repeated measures analysis of variance (ANOVA) for data from tests conducted continuously at different postnatal days, followed by the Student-Newman-Keuls test. Data from gait analysis, immunostaining, and ELISA were presented as the mean±SEM and analyzed by two-way ANOVA followed by the Student-Newman-Keuls test. Results with a $p<0.05$ were considered statistically significant.

Results

rhIGF-1 attenuated LPS-induced motor behavioral deficits

No significant difference was observed between the male and female rats within the same treatment group from P6 to P21. Therefore, data from rats of both sexes were combined and presented here.

Locomotion—Locomotion was measured using the open field test which measures the activity and habituation response of animals on placement in a novel environment [28]. The total distance traveled by the animal, reflected by horizontal activity, increased with age until

P15 in all groups (Fig. 1A). LPS-treatment resulted in hyperactivity from P13 to P17 compared to the control group ($p<0.05$, Fig. 1A). rhIGF-1 treatment significantly decreased the LPS-induced hyperactivity in the LPS+rhIGF-1 group ($p<0.05$, Fig. 1A). However, this behavioral deficit was spontaneously reversible, and at P19 there were no significant differences in horizontal activity between LPS and the control rats (Fig. 1A).

The summation of rearing responses and stereotyped behaviors reflect vertical activity [29]. Neonatal LPS exposure significantly increased the vertical activity at P14 and P21, as indicated by the increased number of rearing events ($p<0.05$, Fig. 1B) at P14 and P21, and stereotyped behaviors at P21 ($p<0.05$, Fig. 1C), compared with the control group. Administration with rhIGF-1 significantly decreased the LPS-induced increase in rearing events and stereotyped responses ($p < 0.05$, Figs. 1B and 1C).

Beam walking test—Consistent with our previous study using the round wood beam [6], all pups from the control group succeeded in the beam walking test by P17, and the beam-walking latency decreased with age ($p<0.05$, Fig. 2A). LPS administration resulted in reduction of success in the beam walking test (all LPS-injected group succeeded on P21), and increase in latency to travel across the round beam ($p<0.05$, Fig. 2A). rhIGF-1 treatment significantly advanced the success in the beam walking test (all of the LPS+rhIGF-1 group succeeded on P19), and improved LPS-induced impaired performance in the beam walking test ($p<0.05$, Fig. 2A).

Gait Analysis—LPS administration resulted in increase in foot length ($p<0.05$, Fig. 2B) and stride width ($p<0.05$, Fig. 2C), and reduction of total spreading (spreading of toes 1–5) ($p<0.05$, Fig. 2B) and stride length ($p<0.05$, Fig. 2C). The gait abnormalities and beam walking deficits have been conducted for evaluation of nigrostriatal lesion in rodent models [31]. rhIGF-1 treatment significantly improved LPS-induced impaired gait performance ($p<0.05$, Figs. 2B & 2C).

rhIGF-1 ameliorated LPS-induced loss of tyrosine hydroxylase-immunoreactive neurons

Positive staining of TH was used to detect dopamine neurons in the SN, VTA and OB. No significant differences in TH and NeuN staining were observed between the ipsilateral (the left) and the contralateral side (right) in the P21 rat brain. Therefore, data from both sides were averaged and presented in the paper. The corresponding intensity profile of TH expression were presented under the photomicrograph of TH+ cells in the different brain regions. Consistent with our previous reports [5, 6], neonatal LPS exposure significantly reduced the number of TH positive neurons in the SN ($p<0.05$, Figs. 3B, 3E & 3G), VTA ($p<0.05$, Figs. 4B, 4E & 4G), and OB of P21 rats ($p<0.05$, Figs. 5B, 5E & 5G) by 44%, 32%, and 22%, respectively. The LPS-induced reduction of TH+ cells were observed at a greater degree in the SN of the P21 rat brain ($p<0.05$, Fig. 6I). However, LPS exposure did not significantly alter the total number of NeuN positive cells (neurons) in the SN (Fig. 3H), VTA (Fig. 4H) and OB (Fig. 5H), suggesting that LPS did not result in actual neuronal cell death in these areas. Therefore, the reduction in the number of TH positive cells may be a consequence of phenotypic suppression of TH expression. rhIGF-1 treatment significantly attenuated the LPS-induced reduction in the number of TH positive neurons in the SN

(p<0.05, Figs. 3C, 3F & 3G), VTA (p<0.05, Figs. 4C, 4F & 4G), and OB of P21 rats (p<0.05, Figs. 5C, 5F & 5G).

LPS-induced chronic inflammation has been found in other central catecholaminergic neurons in the LC of the pons [23, 24]. Therefore, the positive staining of TH in the LC also was determined in the P21 rat brain. LPS exposure significantly reduced the number of TH positive neurons in the LC of P21 rats by 48% (p<0.05, Figs. 6B, 6E & 6G), but did not significantly alter the total number of NeuN positive cells (neurons) in the LC (Fig. 6H). rhIGF-1 treatment significantly attenuated the LPS-induced reduction in the number of TH positive neurons in the LC (p<0.05, Figs. 6C, 6F & 6G).

rhIGF-1 decreased LPS-induced increase in COX-2 expression

Neonatal LPS-induced inflammatory responses can be identified by the increase in the number of COX-2+ cells in the SN (p<0.05, Figs. 7B, 7D, 7G & 7J), VTA, OB and LC of P21 rats (p<0.05, Fig. 7J) compared with the control rats (Figs. 7A & 7J). Double staining showed that most COX-2+ cells in the SN, VTA, OB and LC were co-localized with NeuN+ neurons (Figs. 7F as the example in SN). Some of COX-2+ cells were co-localized with TH + cells (Figs. 7I). The TH+ cells were 36.5±2.58%, 18.8±2.38%, 17.25±1.42%, or 38.3±1.93% co-localized with COX-2+ cells in the SN, VTA, OB and LC, respectively (Fig. 7J). The LPS-induced increase in COX-2+/TH+ cells were observed at a greater degree in the SN and LC of the P21 rat brain (p<0.05). Treatment with rhIGF-1 significantly diminished the increase in the number of COX-2+ cells in the SN, VTA, OB and LC following LPS injection (p<0.05) (Figs. 7C and 7J).

rhIGF-1 suppressed LPS-induced chronic microglia activation

Neonatal LPS exposure resulted in a sustained microglial activation, as indicated by the increased number and features of activated morphology of Iba1+ cells. In the control rat brain, few Iba1+ cells were detected. These detected cells only exhibited resting status, which was characterized by smaller rod shaped soma with fine and ramified processes (Fig. 8A & 8G). A significantly increased number of Iba1+ cells was found in the SN, VTA, OB and LC of the LPS-exposed rat brain (p<0.05, Figs. 8B, 8H and 8J). Moreover, the majority of these Iba1+ cells showed typical features of activated microglia, i.e. bright staining of an elongated or round shaped cell body with blunt or no processes [34] (arrows indicated in Fig. 8B). rhIGF-1 significantly suppressed LPS-induced microglia activation, as shown by the reduced number of Iba1+ cells in the SN (p<0.05, Figs. 8C, 8I and 8J), VTA, OB and LC (p<0.05, Fig. 8J).

rhIGF-1 decreased LPS-induced inflammatory responses

Three major proinflammatory cytokines, IL-1β, IL-6 and TNFα in the SN, VTA, OB and LC of P6 and P21 rat brain were determined by ELISA. LPS induced robust inflammatory responses in the SN, VTA, OB, and LC of P6 rats, as shown by a strong induction of IL-1β and IL-6 levels (Figs. 9A and 9B). The elevation of IL-1β levels in the SN, VTA, OB, and LC was sustained in P21 rats (Fig. 9C), but not for IL-6 levels in the P21 rat brain (data not shown). TNFα was undetectable in the SN, VTA, OB and LC of the P6 and P21 rat brain (data not shown). Administration of rhIGF-1 reduced LPS exposure-induced elevation of

IL-1β levels in all regions at P21 ($p<0.05$, Fig. 9C), but not at P6 (Fig. 9A). However, rhIGF-1 reduced LPS exposure-induced elevation of IL-6 levels in P6 rats ($p<0.05$, Fig. 9B).

Discussion

Perinatal LPS exposure-induced inflammation has been shown to impair neonatal brain development in rats shortly after the exposure and also increase the risk of dopaminergic disorders in animal models of Parkinson's disease [2, 3]. Consistent with the results reported in our previous study [5, 6], neonatal LPS exposure resulted in nigrostriatal dopaminergic neuronal injury (Fig. 3) and such central inflammation also induced neurological dysfunction including locomotion, beam walking test and gait analysis later in life (Figs. 1&2). Gait abnormalities and beam walking deficits have been conducted for evaluation of nigrostriatal lesion in rodent models [31]. Gait disturbances such as gait hypokinesia (reduction in stride length) and motor fluctuations caused by a degeneration of dopaminergic neurons in the SN (the source of dopamine in the nigrostriatal motor pathway) are commonly observed in Parkinson's disease patients [35]. Neonatal LPS exposure impaired the development of locomotor activity in the rat which has been correlated with the maturation of neurotransmitter systems mediating inhibition and excitation [28]. In addition, the increased locomotor activity in the LPS group indicates that these animals may have a delay of accommodation to this experience with repeated exposure to the field [28]. The studies have shown that disorder in locomotor activity is associated with an abnormal level of dopamine content in the rat brain concomitant with SN injury [36]. Moreover, Parkinson's disease is a multisystem disorder, and loss of LC neurons (a source of noradrenaline) also contributes to motor dysfunction in Parkinson's disease [35]. It has been reported that moderate LC damage resulted in reduction of mobility, while extensive LC damage resulted in increase in mobility and correlated with hyperactivity in rodents [24, 37, 38]. The present study shows that neonatal LPS exposure induced chronic inflammation and neuronal injury in the LC area of P21 rats (Fig. 6). Other studies also indicated that LPS treatment leads to brain damage, increases the pro-inflammatory cytokine protein levels and gene expression, and reduces TH immunoreactivity and gene expression in both the SN and LC [23, 24].

Neuronal inflammation has been observed in dopaminergic neurons as evidenced by the co-localization of TH+ and COX-2+ in the SN (Fig. 7). Neonatal LPS exposure produced injury in the nigrostriatal dopaminergic system, as indicated by the phenotypic suppression of TH expression in neurons at the SN of P21 rats (Fig. 3). However, LPS exposure did not alter the total number of NeuN+ neuron (Fig. 3C) and also did not increase the Fluoro-Jade B+ staining, which sensitively and specifically binds to degenerating neurons, (data not shown) in the SN of P21 rats. Therefore, most COX-2+ cells were co-localized with NeuN+, but not all of COX-2+ cells co-localized with TH+ cells in the SN (Fig. 7). Neonatal LPS-induced neuronal damage was also observed in VTA (Fig. 4), OB (Fig. 5) and LC regions of P21 rats (Fig. 6). The current data indicated that dopaminergic neurons in the SN were relatively vulnerable to LPS exposure and resulted in more neuronal inflammation, as indicated by fewer TH+ cells (Fig. 6I) and more COX-2+ cells, than that in the VTA and OB (Fig. 7J). Possible mechanisms that have been reported show that the increased ion levels in SN dopaminergic neurons may enhance vulnerability of SN [39, 40] and higher expression of G-substrate VTA dopaminergic neurons may cause relative protection of VTA [40, 41].

Moreover, altered calcium homeostasis is also suggested to render SN dopaminergic neurons particularly susceptible to degeneration [42]. Neuroinflammation-induced elevated levels of pro-inflammatory cytokines and oxidative stress lead to neuronal Ca+2 dysregulation which may contribute to the selective vulnerability of SN and LC in Parkinson's disease [24, 42, 43]. In addition, destruction of noradrenergic neurons in the LC may precede the damage to the nigral cells which has been suggested to influence the rate of dopaminergic neurons loss in the SN [44].

IGF-1 is the main trophic factor in the central nervous system. It plays an important role during early brain development, including promoting neuronal growth, cellular proliferation, differentiation, myelination, synapse formation, and enhancing secretion of various neurotransmitters in the developing nervous system [8, 9]. The perinatal absence of IGF-1 is lethal and a decrease in IGF-1 may cause brain atrophy, brain abnormalities and loss of neurons [45]. Lower levels of IGF-1 have been reported in different inflammatory conditions in human preterm neonates (sepsis) [46] and LPS treated animals [45, 47]. The insufficient perinatal IGF-1 following LPS may contribute to the brain abnormalities and demyelination. Our previous studies have shown that exposure to LPS in P5 rats resulted in white matter injury and intranasal IGF-1 administration protected against LPS-induced white matter injury and sensorimotor disturbances in the juvenile rat [16]. The present study further demonstrates that intranasal IGF-1 provides protection against neonatal LPS exposure-induced brain dopaminergic (Figs. 3, 4 & 5) and noradrenergic neuronal injury (Fig. 6) and motor behavioral disturbances (Figs. 1 & 2). In addition, it has been reported that IGF-1 is elevated in nigrostriatal dopaminergic neurons (A9), compared to mesocorticolimbic dopaminergic neurons (A10), which may explain the relative vulnerability of A9 to toxins [48].

Our previous study found that IGF-1 co-administered with LPS through intracerebral injection at a low dose (0.5 μg per pup) protects the rat brain from LPS-induced white matter injury [49]. However, some adverse effects such as increased hemorrhage and increased infiltration of polymorphonuclear cells due to the breaking down of BBB were observed following co-injection of IGF-1 with LPS [49]. Intracerebral injection of IGF-1 does not appear to be a practical approach for clinical use due to its invasive nature. Therefore, the non-invasive intranasal treatment approach provides a more practical alternation for IGF-1 administration. No hemorrhage or increased polymorphonuclear cell infiltration was found in the rat brain following intranasal treatment of IGF-1 [16]. The physiological levels of IGF-1 in serum are ~500 ng/ml in rats [50] and the IGF-1 levels in CSF are ~1% of the IGF-1 levels in serum [50]. However, the IGF-1 levels in adult rat olfactory bulbs and in the adolescent rat hippocampus are ~800 pg/mg [51] and ~5 pg/mg [50], respectively. Consistent with our previous study [16], rhIGF-1 administration through intranasal route efficiently penetrated into the rat brain, including olfactory bulbs (~2000 pg/mg), striatum (~1000 pg/mg), and substantia nigra (~500 pg/mg) within 30 minutes (Fig. 1). Mechanisms involved in delivery of IGF-1 through intranasal administration are not yet completely understood. LPS treatment in early life causes a long-term enhancement of BBB permeability and white matter damage in rat [52]. In the current study, no significant differences in rhIGF-1 concentrations were observed between the treatment groups within the respective brain regions, i.e. the concentrations of rhIGF-1 in the same brain region were

not affected by the LPS treatment. This suggests that penetration of intranasally infused rhIGF-1 into the brain might not need to cross the BBB. Furthermore, other studies also indicated that [^{125}I]-IGF-1 is not present in the cisternal CSF in the rat following intranasal administration of [^{125}I]-IGF-1, suggesting that IGF-1 does not have to enter the CSF in order to access the brain [14, 15]. This observation is consistent with other suggestion that intranasal administration may bypass the BBB to deliver and target drugs to the central nervous system along the olfactory and trigeminal neural pathways, reducing systemic exposure and side effects [14, 15].

To further investigate the mechanisms of the neuroprotective effects of IGF-1, neuronal oxidative stress level was measured in the current study. Our results show that neonatal administration of IGF-1 decreased neuronal oxidative stress by suppressing LPS exposure-induced neuronal COX-2 expression in the rat SN, VTA, OB and LC regions at P21 (Fig. 7). Our data also show that IGF-1 treatment reduced neonatal LPS exposure-induced activation of microglia (Fig. 8), and elevation of proinflammatory cytokines such as IL-6 and IL-1β in the SN, VTA, OB and LC regions (Fig. 9). IGF-1 has been shown to modulate neonatal immune responses in maturation processes and inflammation by suppressing pro-inflammatory Th1 cytokine IL-6 and stimulating anti-inflammatory Th2 cytokine IL-10 [53, 54]. Increased IGF-1 production through liposomal IGF-1 gene transfer has been shown to regulate pro- and anti-inflammatory cytokine expression in the burn wound and improve healing, suggesting that IGF-1 decreases local inflammation [55]. It was found that exogenous IGF-1 decreases LPS-induced brain cytokine expression via the down-regulating of glia activation and inducing an endogenous growth factor [12, 13].

IGF-1 is also considered to have a multiple neuroprotective properties, as a result of its autocrine functions in the brain and the control of neuronal excitability, nerve cell metabolism and cell survival [10, 11]. Several studies have shown that intranasally delivered IGF-1 protects against cerebral hypoxic-ischemic injury [17-19], LPS-induced white matter injury in the developing rat brain [16], and other neurodegenerative damages [20, 21] by activation of intracellular signaling cascades such as phophatidylinositol-3 kinase (PI3K)/Akt pathway, which phosphorylates glycogen synthase kinase (GSK)-3β and several other targets critical to cell survival [20, 22]. Activation of PI3K/Akt also leads to reduction of mitochondrial reactive oxygen species (ROS), and enhanced mitochondrial levels of Akt and mitochondrial-encoded complex IV subunit [22]. It has been hypothesized that development of resistance to IGF-1 leads to weakening of neuroprotective signaling and may underlie all of the major pathogenic routes in the central nervous system [10, 56].

In summary, IGF-1 delivered through intranasal route in the neonatal rat provides long-lasting protection against LPS-induced dopaminergic and noradrenergic neuronal injury, and ameliorates LPS-induced motor behavioral dysfunction in juvenile rats. The protective effects of IGF-1 are associated with the decrease in microglia activation and reduction of neuronal oxidative stress by suppressing neuronal COX-2 expression in the rat SN, VTA, OB and LC. Intranasal administration of IGF-1 is a non-invasive method which efficiently delivers IGF-1 into the brain and provides a feasible post-treatment approach for brain injury associated with central inflammation and has potential for great significance in the clinical setting.

Acknowledgments

The authors thank Dr. Rick CS Lin for editing assistance. The authors also thank Prof. Zhengwei Cai and Dr. Suying Lin for their advice on drug administration. This work was supported by NIH grant NIH/NINDS NS080844 (to LW Fan), Newborn Medicine Funds from the Department of Pediatrics, University of Mississippi Medical Center (to LW Fan and Y Pang), grants NSC102-2320-B-030-011 and MOST103-2320-B-030-005-MY3 from the National Science Council of Taiwan (to LT Tien and YJ Lee).

References

1. Raetz CR, Whitfield C. Lipopolysaccharide endotoxins. Annu Rev Biochem. 2002; 71:635–700. [PubMed: 12045108]
2. Fan LW, Tien LT, Lin RC, Simpson KL, Rhodes PG, Cai Z. Neonatal exposure to lipopolysaccharide enhances vulnerability of nigrostriatal dopaminergic neurons to rotenone neurotoxicity in later life. Neurobiol Dis. 2011; 44:304–316. [PubMed: 21798348]
3. Ling Z, Zhu Y, Tong C, Snyder JA, Lipton JW, Carvey PM. Progressive dopamine neuron loss following supra-nigral lipopolysaccharide (LPS) infusion into rats exposed to LPS prenatally. Exp Neurol. 2006; 199:499–512. [PubMed: 16504177]
4. Back SA, Luo NL, Borenstein NS, Levine JM, Volpe JJ, Kinney HC. Late oligodendrocyte progenitors coincide with the developmental window of vulnerability for human perinatal white matter injury. J Neurosci. 2001; 21:1302–1312. [PubMed: 11160401]
5. Fan LW, Pang Y, Lin S, Tien LT, Ma T, Rhodes PG, Cai Z. Minocycline reduces lipopolysaccharide-induced neurological dysfunction and brain injury in the neonatal rat. J Neurosci Res. 2005; 82:71–82. [PubMed: 16118791]
6. Fan LW, Tien LT, Mitchell HJ, Rhodes PG, Cai Z. α-phenyl-*n*-*tert*-butyl-nitrone ameliorates hippocampal injury and improves learning and memory in juvenile rats following neonatal exposure to lipopolysaccharide. Eur J Neurosci. 2008; 27:1475–1484. [PubMed: 18364024]
7. Torres-Aleman I. Toward a Comprehensive Neurobiology of IGF-I. Dev Neurobiol. 2010; 70:384–396. [PubMed: 20186710]
8. Bunn RC, King WD, Winkler MK, Fowlkes JL. Early Developmental Changes in IGF-I, IGF-II, IGF Binding Protein-1, and IGF Binding Protein-3 Concentration in the Cerebrospinal Fluid of Children. Pediatr Res. 2005; 58:89–93. [PubMed: 15774848]
9. Fernandez AM, Torres-Aleman I. The many faces of insulin-like peptide signalling in the brain. Nat Rev Neurosci. 2012; 13:225–239. [PubMed: 22430016]
10. Bassil F, Fernagut PO, Bezard E, Meissner WG. Insulin, IGF-1 and GLP-1 signaling in neurodegenerative disorders: targets for disease modification? Prog Neurobiol. 2014; 118:1–18. [PubMed: 24582776]
11. Zemva J, Schubert M. The role of neuronal insulin/insulin-like growth factor-1 signaling for the pathogenesis of Alzheimer's disease: possible therapeutic implications. CNS Neurol Disord Drug Targets. 2014; 13:322–337. [PubMed: 24059318]
12. Park SE, Lawson M, Dantzer R, Kelley K. McCusker RH: Insulin-like growth factor-I peptides act centrally to decrease depression-like behavior of mice treated intraperitoneally with lipopolysaccharide. J Neuroinflammation. 2011; 8:179. [PubMed: 22189158]
13. Sukhanov S, Higashi Y, Shai SY, Vaughn C, Mohler J, Li Y, Song YH, Titterington J, Delafontaine P. IGF-1 reduces inflammatory responses, suppresses oxidative stress, and decreases atherosclerosis progression in ApoE-deficient mice. Arterioscler Thromb Vasc Biol. 2007; 27:2684–2690. [PubMed: 17916769]
14. Hanson LR, Frey WH 2nd. Intranasal delivery bypasses the blood-brain barrier to target therapeutic agents to the central nervous system and treat neurodegenerative disease BMC Neurosci. 2008; 9:S5. [PubMed: 19091002]
15. Thorne RG, Pronk GJ, Padmanabhan V, Frey WH 2nd. Delivery of insulin-like growth factor-I to the rat brain and spinal cord along olfactory and trigeminal pathways following intranasal administration. Neuroscience. 2004; 127:481–496. [PubMed: 15262337]

16. Cai Z, Fan LW, Lin S, Pang Y, Rhodes PG. Intranasal administration of insulin-like growth factor-1 protects against lipopolysaccharide-induced injury in the developing rat brain. Neuroscience. 2011; 194:195–207. [PubMed: 21840378]
17. Lin S, Fan LW, Rhodes PG, Cai Z. Intranasal administration of IGF-1 attenuates hypoxic-ischemic brain injury in neonatal rats. Exp Neurol. 2009; 217:361–370. [PubMed: 19332057]
18. Liu XF, Fawcett JR, Hanson LR, Frey WH 2nd. The window of opportunity for treatment of focal cerebral ischemic damage with noninvasive intranasal insulin-like growth factor-I in rats. J Stroke Cerebrovasc Dis. 2004; 13:16–23. [PubMed: 17903945]
19. Wood TL, Loladze V, Altieri S, Gangoli N, Levison SW, Brywe KG, Mallard C, Hagberg H. Delayed IGF-1 administration rescues oligodendrocyte progenitors from glutamate-induced cell death and hypoxic-ischemic brain damage. Dev Neurosci. 2007; 29:302–310. [PubMed: 17762198]
20. Lopes C, Ribeiro M, Duarte AI, Humbert S, Saudou F, Pereira de Almeida L, Hayden M, Rego AC. IGF-1 intranasal administration rescues Huntington's disease phenotypes in YAC128 mice. Mol Neurobiol. 2014; 49:1126–1142. [PubMed: 24347322]
21. Vig PJ, Subramony SH, D'Souza DR, Wei J, Lopez ME. Intranasal administration of IGF-I improves behavior and Purkinje cell pathology in SCA1 mice. Brain Res Bull. 2006; 69:573–579. [PubMed: 16647585]
22. Ribeiro M, Rosenstock TR, Oliveira AM, Oliveira CR, Rego AC. Insulin and IGF-1improve mitochondrial functionin a PI-3K/Akt-dependent manner and reduce mitochondrial generation of reactive oxygen species in Huntington's disease knock-in striatal cells. Free Radic Biol Med. 2014; 74:129–144. [PubMed: 24992836]
23. Bardou I, Kaercher RM, Brothers HM, Hopp SC, Royer S, Wenk GL. Age and duration of inflammatory environment differentially affect the neuroimmune response and catecholaminergic neurons in the midbrain and brainstem. Neurobiol Aging. 2014; 35:1065–1073. [PubMed: 24315728]
24. Hopp SC, Royer SE, D'Angelo HM, Kaercher RM, Fisher DA, Wenk GL. Differential neuroprotective and anti-inflammatory effects of L-type voltage dependent calcium channel and ryanodine receptor antagonists in the substantia nigra and locus coeruleus. J Neuroimmune Pharmacol. 2015; 10:35–44. [PubMed: 25318607]
25. Straley ME, Van Oeffelen W, Theze S, Sullivan AM, O'Mahony SM, Cryan JF, O'Keeffe GW. Distinct alterations in motor & reward seeking behavior are dependent on the gestational age of exposure to LPS-induced maternal immune activation. Brain Behav Immun. 2016; (16):S0889–1591. 30151–9.
26. He Q, Li YH, Guo SS, Wang Y, Lin W, Zhang Q, Wang J, Ma CG, Xiao BG. Inhibition of Rho-kinase by Fasudil protects dopamine neurons and attenuates inflammatory response in an intranasal lipopolysaccharide-mediated Parkinson's model. Eur J Neurosci. 2016; 43:41–52. [PubMed: 26565388]
27. Kirsten TB, Chaves GP, Taricano M, Martins DO, Flório JC, Britto LR, Torrão AS, Palermo-Neto J, Bernardi MM. Prenatal LPS exposure reduces olfactory perception in neonatal and adult rats. Physiol Behav. 2011; 104:417–422. [PubMed: 21570993]
28. Hermans RH, Hunter DE, McGivern RF, Cain CD, Longo LD. Behavioral sequelae in young rats of acute intermittent antenatal hypoxia. Neurotoxicol Teratol. 1992; 14:119–129. [PubMed: 1593986]
29. Antoniou K, Papathanasiou G, Panagis G, Nomikos GG, Hyphantis T, Papadopoulou-Daifoti Z. Individual responses to novelty predict qualitative differences in d-amphetamine-induced open field but not reward-related behaviors in rats. Neuroscience. 2004; 123:613–623. [PubMed: 14706774]
30. Karl T, Pabst R, von Horsten S. Behavioral phenotyping of mice in pharmacological and toxicological research. Exp Toxicol Pathol. 2003; 55:69–83. [PubMed: 12940631]
31. Westin JE, Janssen ML, Sager TN, Temel Y. Automated gait analysis in bilateral parkinsonian rats and the role of L-DOPA therapy. Behav Brain Res. 2012; 226:519–528. [PubMed: 22008381]

32. Pang Y, Lin S, Wright C, Shen J, Carter K, Bhatt A, Fan LW. Intranasal insulin protects against substantial nigra dopaminergic neuronal loss and alleviates motor deficits induced by 6-OHDA in rats. Neuroscience. 2016; 318:157–165. [PubMed: 26777890]
33. Gundersen HJG, Jensen EB. The efficiency of systematic sampling in stereology and its prediction. J Microsc. 1987; 147:229–263. [PubMed: 3430576]
34. Kreutzberg GW. Microglia: a sensor for pathological events in the CNS. Trends Neurosci. 1996; 19:312–318. [PubMed: 8843599]
35. Devos D, Defebvre L, Bordet R. Dopaminergic and non-dopaminergic pharmacological hypotheses for gait disorders in Parkinson's disease. Fundam Clin Pharmacol. 2010; 24:407–421. [PubMed: 20163480]
36. Bakos J, Duncko R, Makatsori A, Pirnik Z, Kiss A, Jezova D. Prenatal immune challenge affects growth, behavior, and brain dopamine in offspring. Ann NY Acad Sci. 2004; 1018:281–287. [PubMed: 15240379]
37. Harro J, Pahkla R, Modiri AR, Harro M, Kask A, Oreland L. Dose-dependent effects of noradrenergic denervation by DSP-4 treatment on forced swimming and beta-adrenoceptor binding in the rat. J Neural Transm. 1999; 106:619–629. [PubMed: 10907722]
38. Stone EA, Lin Y, Sarfraz Y, Quartermain D. The role of the central noradrenergic system in behavioral inhibition. Brain Res Rev. 2011; 67:193–208. [PubMed: 21315760]
39. Dutta D, Ali N, Banerjee E, Singh R, Naskar A, Paidi RK, Mohanakumar KP. Low Levels of Prohibitin in Substantia Nigra Makes Dopaminergic Neurons Vulnerable in Parkinson's Disease. Mol Neurobiol. 2017; doi: 10.1007/s12035-016-0328-y.
40. Lv Z, Jiang H, Xu H, Song N, Xie J. Increased iron levels correlate with the selective nigral dopaminergic neuron degeneration in Parkinson's disease. J Neural Transm. 2011; 118:361–369. [PubMed: 20556443]
41. Chung CY, Koprich JB, Endo S, Isacson O. An endogenous serine/threonine protein phosphatase inhibitor, G-substrate, reduces vulnerability inmodels of Parkinson's disease. J Neurosci. 2007; 27:8314–8323. [PubMed: 17670978]
42. Surmeier DJ, Schumacker PT. Calcium, bioenergetics, and neuronal vulnerability in Parkinson's disease. J Biol Chem. 2013; 288:10736–10741. [PubMed: 23086948]
43. Mattson MP. Parkinson's disease: don't mess with calcium. J Clin Invest. 2012; 122:1195–1198. [PubMed: 22446181]
44. Del Tredici K, Braak H. Dysfunction of the locus coeruleus-norepinephrine system and related circuitry in Parkinson's disease-related dementia. J Neurol Neurosurg Psychiatry. 2013; 84:774–783. [PubMed: 23064099]
45. Szczesny E, Basta-Kaim A, Slusarczyk J, Trojan E, Glombik K, Regulska M, Leskiewicz M, Budziszewska B, Kubera M, Lason W. The impact of prenatal stress on insulin-like growth factor-1 and pro-inflammatory cytokine expression in the brains of adult male rats: The possible role of suppressors of cytokine signaling proteins. J Neuroimmunol. 2014; 276:37–46. [PubMed: 25151093]
46. Perez-Munuzuri A, Couce-Pico ML, Bana-Souto A, Lopez-Suarez O, Iglesias-Deus A, Blanco-Teijeiro J, Fernandez-Lorenzo JR, Fraga-Bermudez JM. Preclinical screening for retinopathy of prematurity risk using IGF1 levels at 3 weeks post-partum. PLoS One. 2014; 9:e88781. [PubMed: 24523937]
47. Priego T, Granado M, Ibanez de Caceres I, Martin AI, Villanua MA, Lopez-Calderon A. Endotoxin at low doses stimulates pituitary GH whereas it decreases IGF-I and IGF-binding protein-3 in rats. J Endocrinol. 2003; 179:107–117. [PubMed: 14529571]
48. Chung CY, Seo H, Sonntag KC, Brooks A, Lin L, Isacson O. Cell type-specific gene expression of midbrain dopaminergic neurons reveals molecules involved in their vulnerability and protection. Hum Mol Genet. 2005; 14:1709–1725. [PubMed: 15888489]
49. Pang Y, Zheng B, Campbell L, Fan LW, Cai Z, Rhodes PG. IGF-1 can either protect or deteriorate LPS-induced damage to the developing rat brain. Pediatr Res. 2010; 67:579–584. [PubMed: 20220546]

50. Yan H, Mitschelen M, Bixler GV, Brucklacher RM, Farley JA, Han S, Freeman WM, Sonntag WE. Circulating IGF1 regulates hippocampal IGF1 levels and brain gene expression during adolescence. J Endocrinol. 2011; 211:27–37. [PubMed: 21750148]

51. Trojan E, Głombik K, Slusarczyk J, Budziszewska B, Kubera M, Roman A, Lason W, Basta-Kaim A. The beneficial impact of antidepressant drugs on prenatal stress-evoked malfunction of the insulin-like growth factor-1 (IGF-1) protein family in the olfactory bulbs of adult rats. Neurotox Res. 2016; 29:288–298. [PubMed: 26610812]

52. Stolp HB, Dziegielewska KM, Ek CJ, Potter AM, Saunders NR. Long-term changes in blood-brain barrier permeability and white matter following prolonged systemic inflammation in early development in the rat. Eur J Neurosci. 2005; 22:2805–2816. [PubMed: 16324115]

53. Kooijman R, Coppens A. Insulin-like growth factor-I stimulates IL-10 production in human T cells. J Leuk Biol. 2004; 76:862–867.

54. Law HKW, Tu W, Liu E, Lau YL. Insulin-like growth factor I promotes cord blood T cell maturation through monocytes and inhibits their apoptosis in part through interleukin-6. BMC Immunol. 2008; 9:74. [PubMed: 19091070]

55. Spies M, Nesic O, Barrow RE, Perez-Polo JR, Herndon DN. Liposomal IGF-1 gene transfer modulates pro- and anti-inflammatory cytokine mRNA expression in the burn wound. Gene Therapy. 2001; 8:1409–1415. [PubMed: 11571581]

56. Torres-Aleman I. Insulin-Like Growth Factor-1 and Central Neurodegenerative Diseases. Endocrinol Metab Clin North Am. 2012; 41:395–408. [PubMed: 22682637]

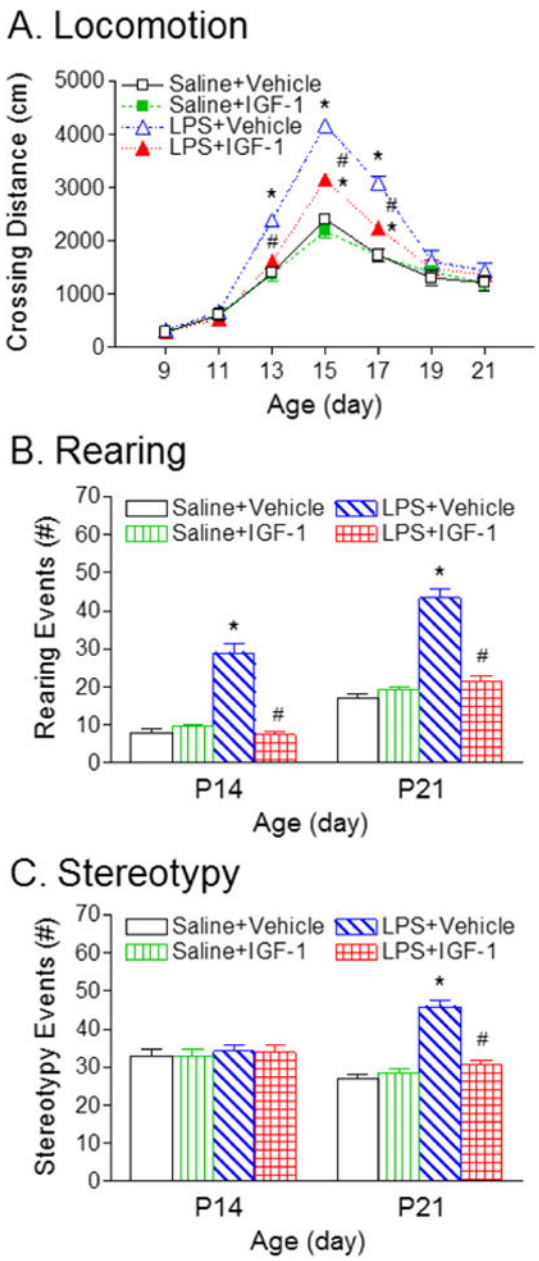

Fig. 1.

rhIGF-1 attenuated LPS-induced deficits in locomotor and stereotyped behaviors, as determined by the open field test (crossing distance) (A), total rearing events (B), and stereotyped behaviors (C) of rats. LPS treatment resulted in hyperactivity, whereas rhIGF-1 treatment decreased the LPS-induced hyperactivity in the LPS+rhIGF-1 group. The results are expressed as the mean+SEM of twelve animals in each group and analyzed by two-way repeated measures ANOVA for data from tests conducted continuously at different postnatal days, followed by the Student-Newman-Keuls test. *P<0.05 represents significant difference for the LPS+Vehicle group or LPS+IGF-1 group compared with the Saline+Vehicle group. #P<0.05 represents significant difference for the LPS+IGF-1 group compared with the LPS +Vehicle group.

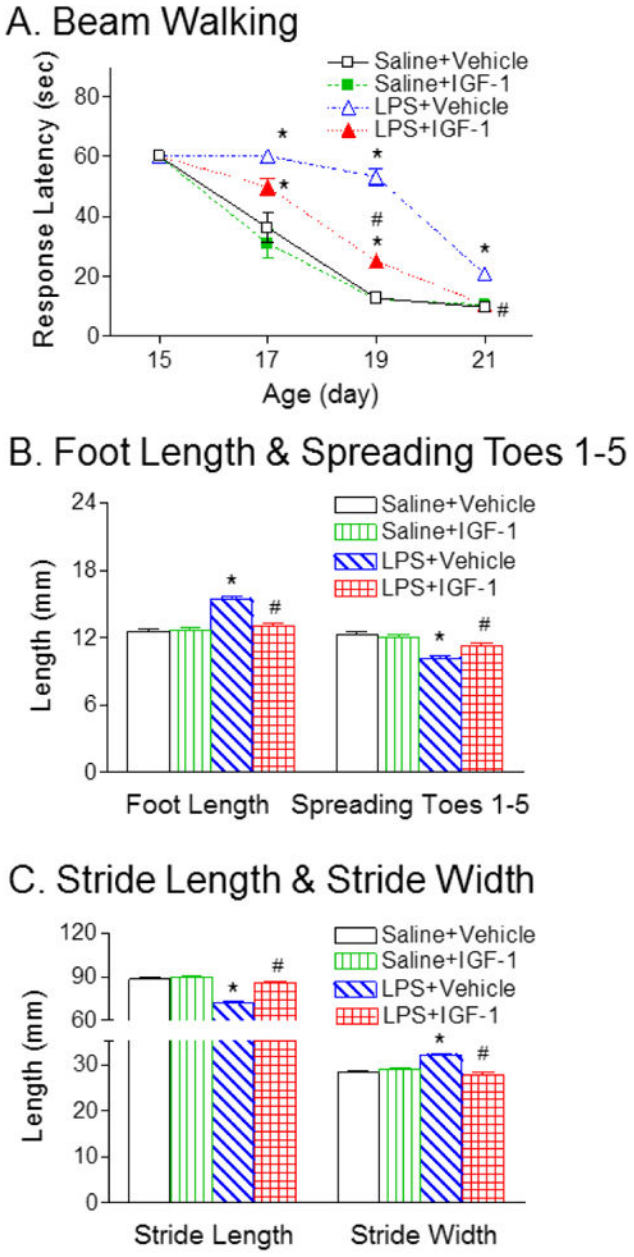

Fig. 2.

rhIGF-1 attenuated LPS-induced deficits in beam walking test (A) and gait analysis, as determined by the foot length and spreading of toes 1-5 (B), and stride length and stride width (C) of rats. LPS treatment resulted in increase in latency to travel across the round beam and rhIGF-1 treatment improved LPS-induced impaired performance in the beam walking test. LPS treatment also caused gait abnormalities, as indicated by increase in foot length and stride width, and reduction of total spreading (spreading of toes 1-5) and stride length. rhIGF-1 treatment improved LPS-induced impaired gait performance. The results are expressed as the mean+SEM of twelve animals in each group and analyzed by two-way repeated measures ANOVA for data from tests conducted continuously at different postnatal days or two-way ANOVA, followed by the Student-Newman-Keuls test. *P<0.05 represents

significant difference for the LPS+Vehicle group or LPS+IGF-1 group compared with the Saline+Vehicle group. #P<0.05 represents significant difference for the LPS+IGF-1 group compared with the LPS+Vehicle group.

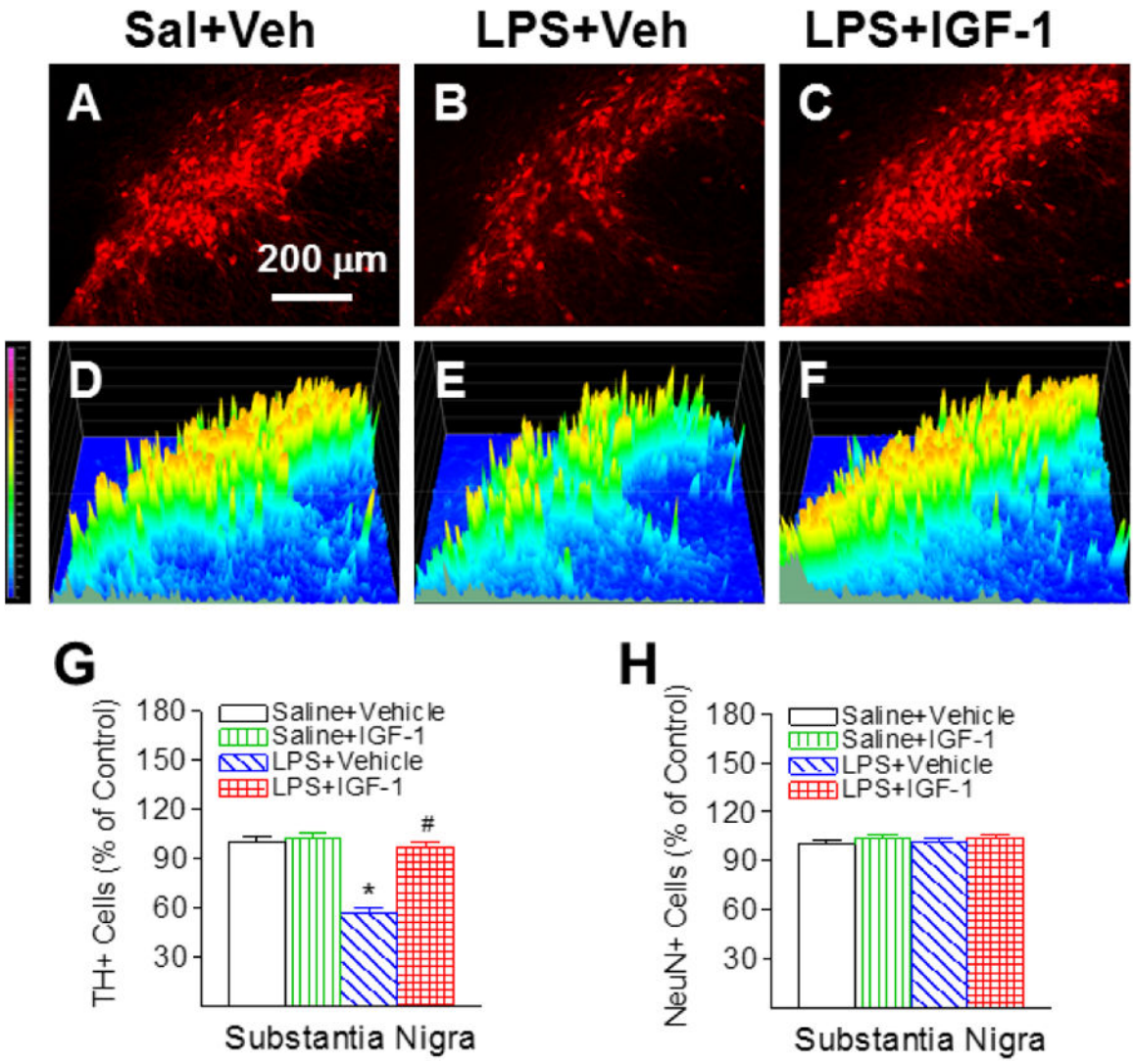

Fig. 3.

rhIGF-1 attenuated neonatal LPS-induced reduction in the number of TH+ cells in the substantia nigra (SN) of the P21 rat brain. Representative photomicrographs of TH+ neurons in the SN region for the Saline+Vehicle group (A), the LPS+Vehicle group (B), and the LPS +IGF-1 group (C). The corresponding intensity profiles of TH expression were presented under the photomicrographs of TH+ cells in the SN region (D-F). LPS injection resulted in a loss of TH+ staining (B&E). rhIGF-1 attenuated LPS-induced loss of TH+ staining (C&F). Quantification of TH+ cells and NeuN+ cells in the SN are shown in G and H, respectively. The results are expressed as the mean+SEM of six animals in each group and analyzed by two-way ANOVA, followed by the Student-Newman-Keuls test. *$P<0.05$ represents significant difference for the LPS+Vehicle group compared with the Saline+Vehicle group. $^{\#}P<0.05$ represents significant difference for the LPS+IGF-1 group compared with the LPS +Vehicle group.

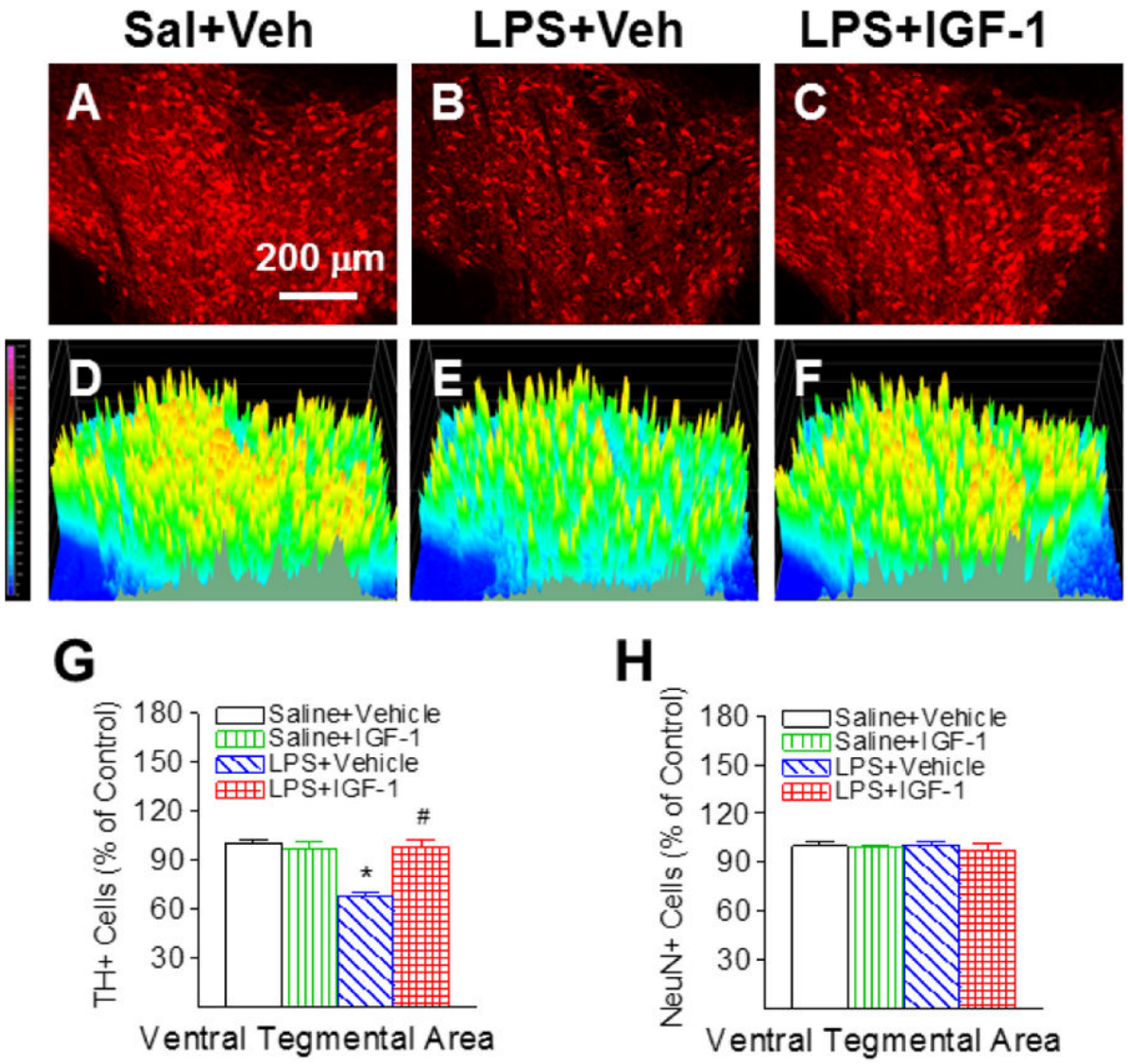

Fig. 4.

rhIGF-1 attenuated neonatal LPS-induced reduction in the number of TH+ cells in the ventral tegmental area (VTA) of the P21 rat brain. Representative photomicrographs of TH+ neurons in the VTA region for the Saline+Vehicle group (A), the LPS+Vehicle group (B), and the LPS+IGF-1 group (C). The corresponding intensity profiles of TH expression were presented under the photomicrographs of TH+ cells in the VTA region (D-F). LPS injection resulted in a loss of TH+ staining (B&E). rhIGF-1 attenuated LPS-induced loss of TH+ staining (C&F). Quantification of TH+ cells and NeuN+ cells in the VTA are shown in G and H, respectively. The results are expressed as the mean+SEM of six animals in each group and analyzed by two-way ANOVA, followed by the Student-Newman-Keuls test. *$P<0.05$ represents significant difference for the LPS+Vehicle group compared with the Saline+Vehicle group. $^{\#}P<0.05$ represents significant difference for the LPS+IGF-1 group compared with the LPS+Vehicle group.

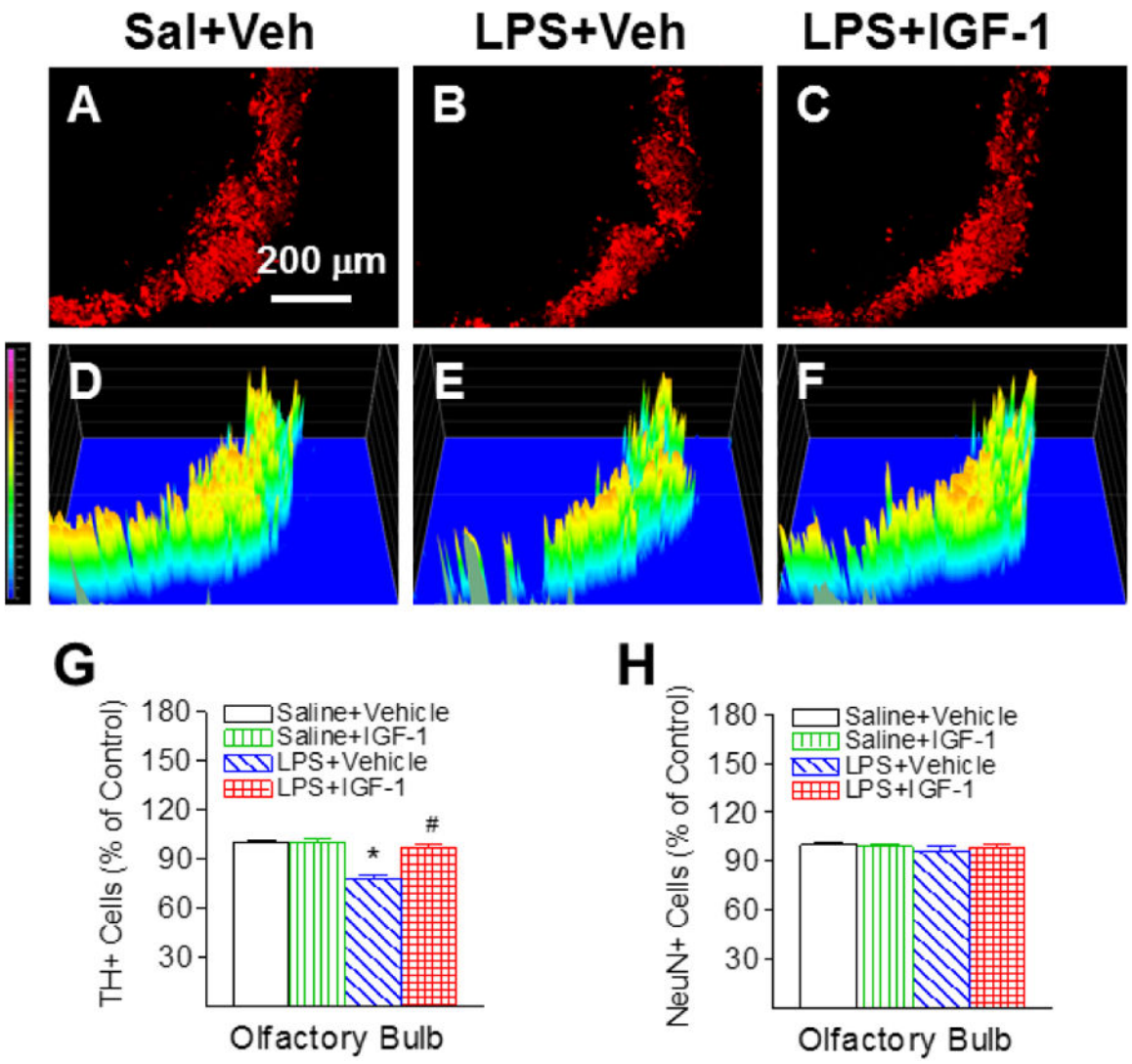

Fig. 5.

rhIGF-1 attenuated neonatal LPS-induced reduction in the number of TH+ cells in the olfactory bulb (OB) of the P21 rat brain. Representative photomicrographs of TH+ neurons in the OB region for the Saline+Vehicle group (A), the LPS+Vehicle group (B), and the LPS +IGF-1 group (C). The corresponding intensity profiles of TH expression were presented under the photomicrographs of TH+ cells in the OB region (D-F). LPS injection resulted in a loss of TH+ staining (B&E). rhIGF-1 attenuated LPS-induced loss of TH+ staining (C&F). Quantification of TH+ cells and NeuN+ cells in the OB are shown in G and H, respectively. The results are expressed as the mean+SEM of six animals in each group and analyzed by two-way ANOVA, followed by the Student-Newman-Keuls test. *$P<0.05$ represents significant difference for the LPS+Vehicle group compared with the Saline+Vehicle group. #$P<0.05$ represents significant difference for the LPS+IGF-1 group compared with the LPS +Vehicle group.

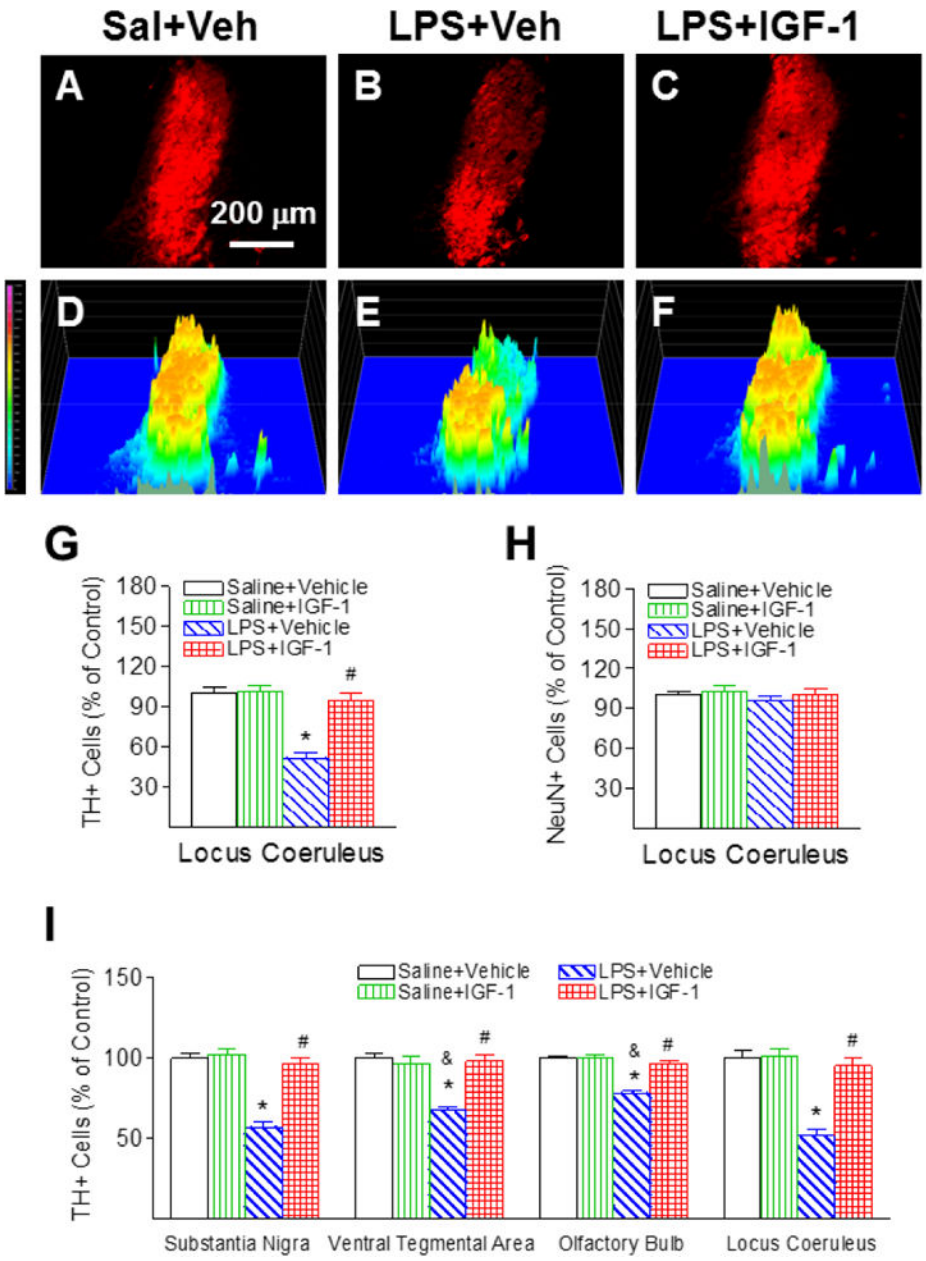

Fig. 6.

rhIGF-1 attenuated neonatal LPS-induced reduction in the number of TH+ cells in the locus coeruleus (LC) of the P21 rat brain. Representative photomicrographs of TH+ neurons in the VTA region for the Saline+Vehicle group (A), the LPS+Vehicle group (B), and the LPS +IGF-1 group (C). The corresponding intensity profiles of TH expression were presented under the photomicrographs of TH+ cells in the LC region (D-F). LPS injection resulted in a loss of TH+ staining (B&E). rhIGF-1 attenuated LPS-induced loss of TH+ staining (C&F). Quantification of TH+ cells and NeuN+ cells in the LC are shown in G and H, respectively. Quantification of the TH+ cells in the SN, VTA, OB and LC are shown in I. The results are expressed as the mean+SEM of six animals in each group and analyzed by two-way ANOVA, followed by the Student-Newman-Keuls test. *P<0.05 represents significant

difference for the LPS+Vehicle group compared with the Saline+Vehicle group. #P<0.05 represents significant difference for the LPS+IGF-1 group compared with the LPS+Vehicle group. &P<0.05 represents significant difference for the LPS+Vehicle group in VTA or OB regions compared with the LPS+Vehicle group in the SN.

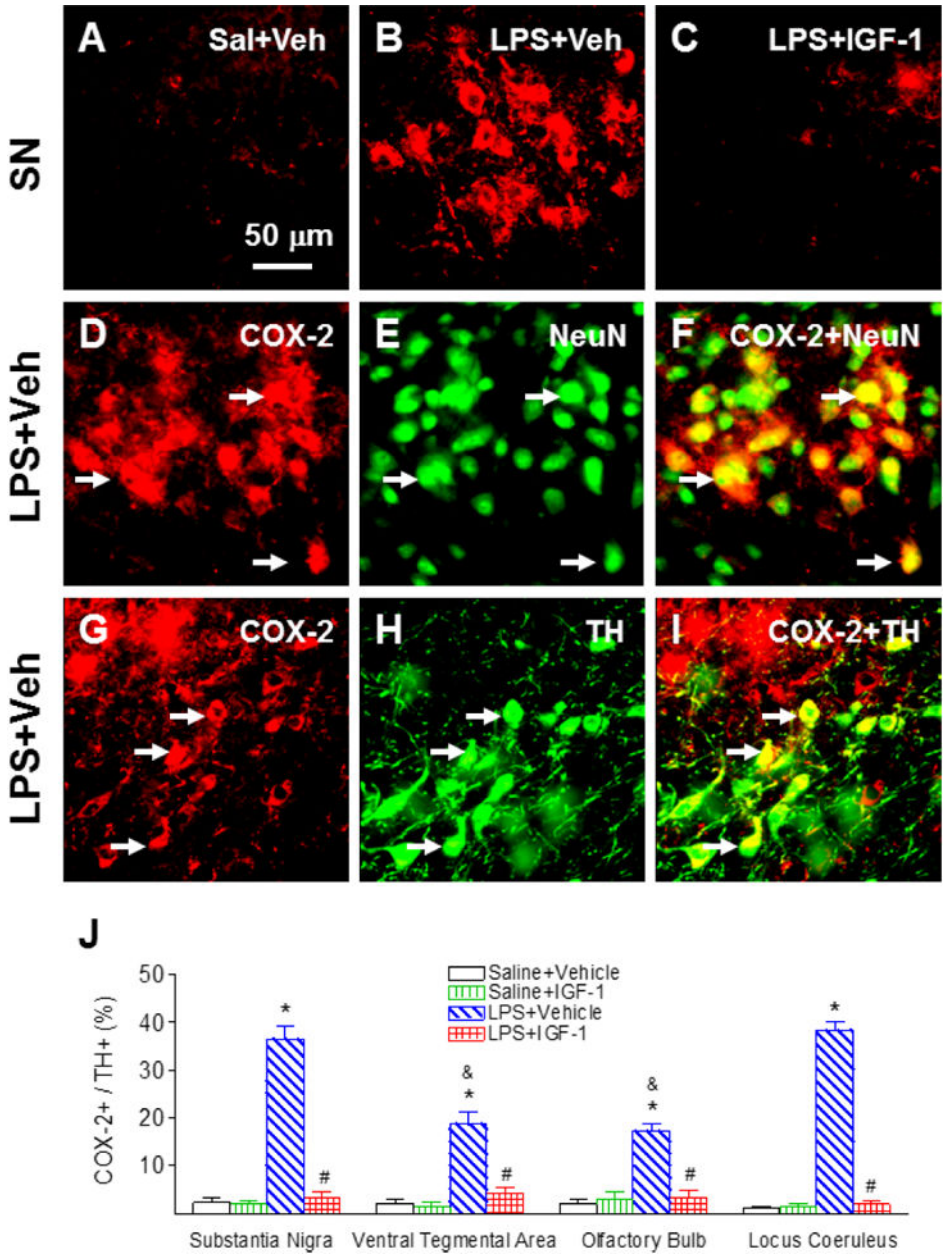

Fig. 7.

rhIGF-1 attenuated neonatal LPS-induced increase in the expression of inducible cyclooxygenase, as indicated by COX-2+ staining in the SN of the P21 rat brain. Representative photomicrographs of COX-2+ (red, A-C, D, G), NeuN+ cells (green, E), TH + cells (green, H), COX-2+ and NeuN+ (yellow, F) or COX-2+ and TH+ double-labeled cells (yellow, I). Double-labeling (yellow, F) showed that most COX-2+ cells (D) were NeuN+ cells (neurons) (E, green). Some COX-2+ cells (yellow, I) were double-labeled with TH+ cells (H, green). Quantification of the ratio of COX-2+ cells to TH+ cells in the SN, VTA, OB and LC are shown in J. The results are expressed as the mean+SEM of six animals in each group and analyzed by two-way ANOVA, followed by the Student-Newman-Keuls test. *P<0.05 represents significant difference for the LPS+Vehicle group compared with the

Saline+Vehicle group. #P<0.05 represents significant difference for the LPS+IGF-1 group compared with the LPS+Vehicle group. &P<0.05 represents significant difference for the LPS+Vehicle group in VTA or OB regions compared with the LPS+Vehicle group in the SN.

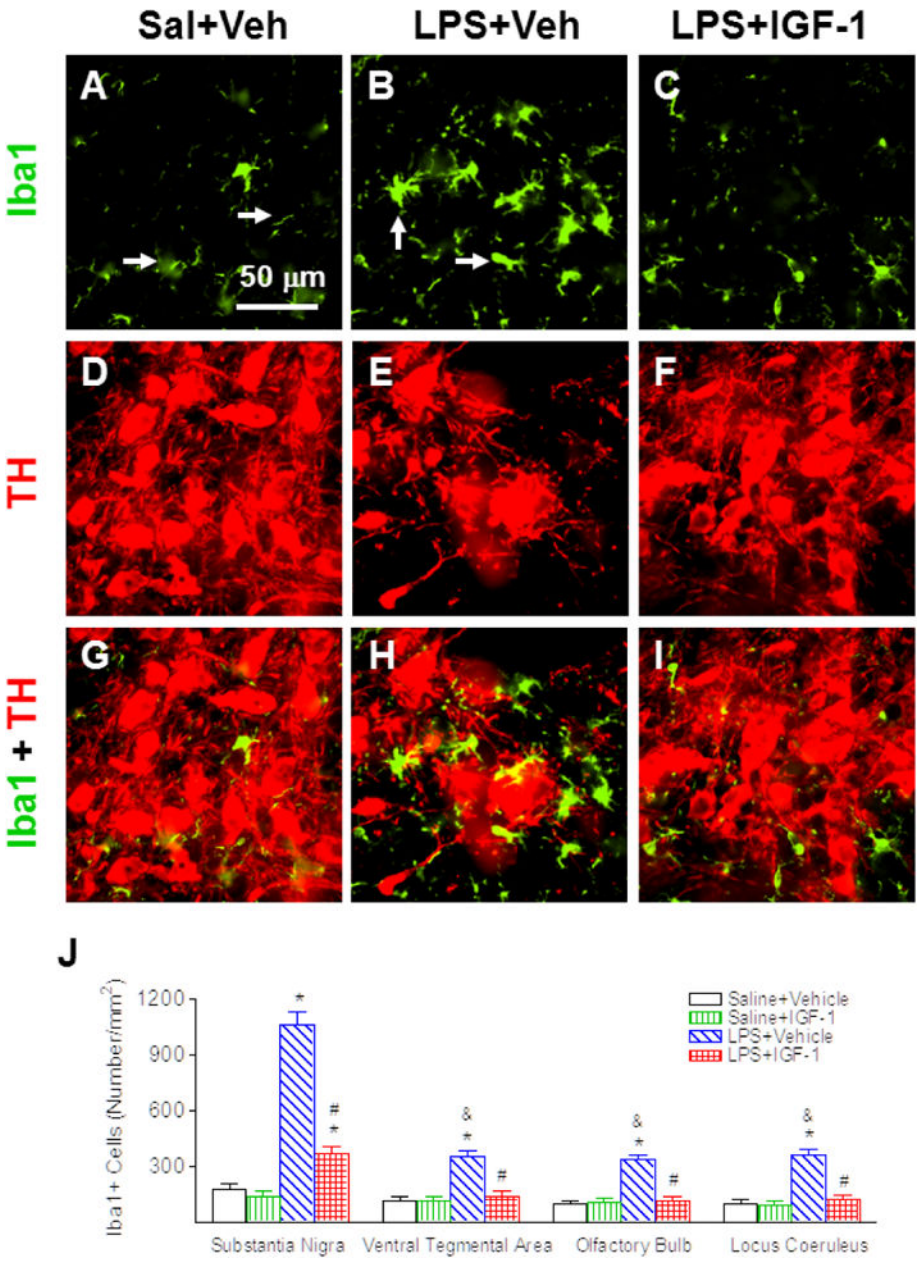

Fig. 8.

rhIGF-1 reduced neonatal LPS-induced microglia activation, as assessed by Iba1+ staining in the SN of the P21 rat brain. Representative photomicrographs of Iba1+ cells (green, A-C), TH+ cells (red, D-F), and merged images for Iba1+ and TH+ cells (G-I) in the SN. Most microglia were in a resting state with a ramified shape (arrow indicated in A) in the rat brain of the Saline+Vehicle group (A). LPS exposure induced the increase of numerous activated microglia with enlarged cell bodies and blunt processes (B & H; arrows indicated in B). rhIGF-1 attenuated LPS-induced increase in activated microglia (C & I). Microglia activation was quantified by counting the number of Iba1+ cells in the SN, VTA, OB and LC (J). The results are expressed as the mean+SEM of six animals in each group and analyzed by two-way ANOVA, followed by the Student-Newman-Keuls test. *P<0.05 represents

significant difference for the LPS+Vehicle group or LPS+IGF-1 group compared with the Saline+Vehicle group. #P<0.05 represents significant difference for the LPS+IGF-1 group compared with the LPS+Vehicle group. &P<0.05 represents significant difference for the LPS+Vehicle group in VTA, OB, or LC regions compared with the LPS+Vehicle group in the SN.

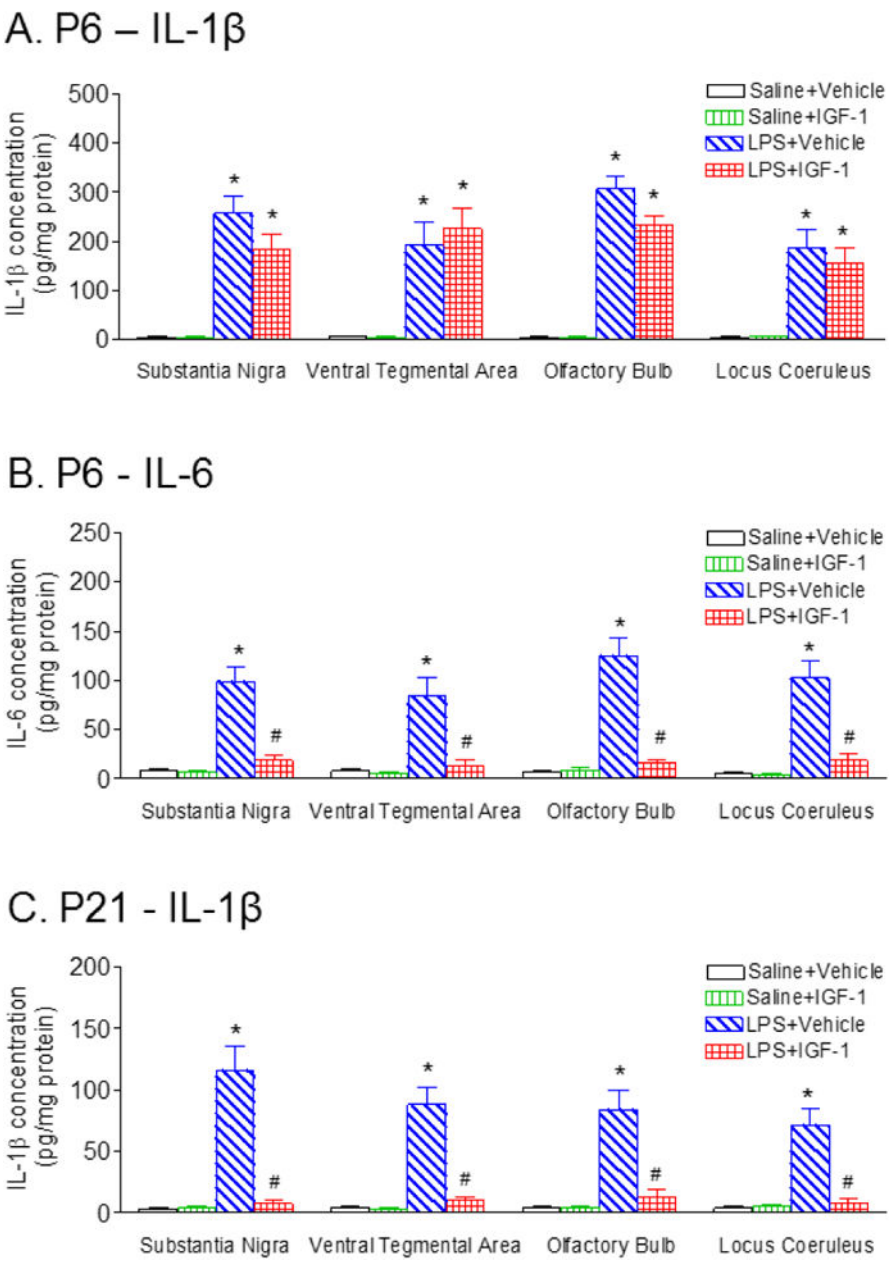

Fig. 9.

rhIGF-1 attenuated the LPS exposure-induced increases in cytokines in the SN, VTA and LC of the rat 1 day (P6) and 16 days (P21) following LPS injection. The concentration levels of IL-1β 1 day (P6) (A), or 16 days (P21) (C) following LPS injection in the SN, VTA and LC were elevated compared with the control group. rhIGF-1 attenuated LPS-induced increase in the concentration levels of IL-1β in the SN, VTA, OB and LC of P21 rats (C). B, At one day (P6) following LPS injection, the concentration of IL-6 in the SN, VTA, OB and LC was elevated compared with the control group, but not in the P21 rat. rhIGF-1 attenuated LPS-induced increase in the concentration levels of IL-6 in the SN, VTA, OB and LC of P6 rats. The results are expressed as the mean±SEM of six animals in each group and analyzed by two-way ANOVA, followed by the Student-Newman-Keuls test. *P<0.05 represents

significant difference for the LPS+Vehicle group or LPS+IGF-1 group compared with the Saline+Vehicle group. #P<0.05 represents significant difference for the LPS+IGF-1 group compared with the LPS+Vehicle group.